# Atmospheric Response to Variations in Sea Surface Temperature[1,2]

by

Jerome Spar[3] and Robert Atlas

The City College, CUNY

New York, N. Y. 10031



October 1974

[1] This research was supported by the National Aeronautics and Space Administration (NASA), Goddard Space Flight Center, under Grant NGR 33-013-086.

[2] Contribution No. 37, University Institute of Oceanography, City University of New York.

[3] Department of Earth and Planetary Sciences.

## Abstract

An extended range prediction experiment was performed with the GISS atmospheric model on a global data set beginning 20 December 1972 to test the sensitivity of the model to sea surface temperature (SST) variation over a two-week forecast period. The use of an initial observed SST field in place of the climatological monthly mean sea temperatures for surface flux calculations in the model is found to have a significant effect on the predicted precipitation over the ocean, with enhanced convection computed over areas where moderately large warm SST anomalies are found. However, there is no detectable positive effect of the SST anomaly field on forecast quality. The influence of the SST anomalies on the daily predicted fields of pressure and geopotential is relatively insignificant up to about one week compared with the growth of prediction error, and is no greater over a two-week period than that resulting from random errors in the initial meteorological state. The 14-day average fields of sea level pressure and 500-mb height predicted by the model, appear to be similarly insensitive to anomalies of sea surface temperature.

## Introduction

The oceans and atmosphere interact in a complex manner through exchanges of mass, momentum, and energy across the air-sea interface on all space and time scales. The complete physical consequences of these interactions for both the sea and the air can ultimately be calculated only through the use of coupled air-sea models (e.g., Manabe and Bryan, 1969) in which each fluid is free to respond to the influence of the other. However, as such interactive models are still in a rather early stage of development, it may be some time before reliable calculations of this kind become available.

Although dependable coupled air-sea models are not yet available for this purpose, it is nevertheless possible to calculate the atmospheric response to variations in the physical state of the sea surface with non-interactive atmospheric models in which the sea surface parameters are specified rather than predicted. Vertical fluxes of water vapor, heat, and momentum across the sea-air interface in both short-range prediction and general circulation models are commonly computed from "bulk aerodynamic" parameterizations, generally with some form of dependence of the exchange coefficients on surface wind and static stability. A major meteorological objective of the interactive models is to provide the correct sea surface temperature (SST) fields for the time-dependent surface flux calculations. In computations with non-interactive atmospheric models, the SST field must, of course, be specified, although it may also be allowed to vary in time.

A number of computational experiments have already been carried out with various weather prediction and general circulation models, to evaluate the influence of SST variations on the behavior of the atmosphere. One group of experiments, notably those by Rowntree (1972), Spar (1973), and Houghton, et al. (1974) was inspired by several speculative and empirical studies regarding the influence of persistent, large-scale SST anomalies on the evolution of the atmosphere over long time periods (of the order of months) and their relevance to long-range weather prediction. (See, e.g., Bjerknes, 1966, 1969; Namias, 1962, 1969, 1970, 1971; Ratcliffe, 1973; Sawyer, 1965; White and Walker, 1973.) These computations have shown that persistent and coherent large scale deviations of sea temperatures from the climatological normals, through their effects on the surface fluxes, may indeed generate significant remote, as well as local, atmospheric reactions over periods of time from a month to a season. However, the results do not necessarily indicate that SST anomalies provide a practical basis for dynamical long-range weather prediction. On the contrary, there appears to be nc physical reason to expect that the atmosphere is any more predictable when SST anomalies exist than when they do not, and in fact some of the experiments suggest (Spar, 1973, c) that unpredicted sea temperature variations may constitute an important source of indeterminacy for the atmosphere.

The importance of surface fluxes over the oceans for short-range weather prediction has also been recognized for many years. Indeed, a number of experiments were performed with early filtered baroclinic models to test the effects of diabatic processes, including surface heat flux as well as latent heat release, on forecast quality, particularly with respect to the prediction of cyclogenesis. (See, e.g., Bushby and Hinds, 1955; Reed, 1958; Spar, et al. 1961; Spar, 1962; Japan Meteorological Agency, 1965.) As in the long-range forecast experiments, the method commonly used is a comparison of two (or more) parallel forecasts started from identical initial meteorological conditions. In the long range forecast experiments, the parallel predictions were computed using, alternately, climatological and anomalous SST fields. (The former computation is sometimes referred to as a "control" run and the latter as an "anomaly" run.) In the early short-range experiments, the parallel forecasts were generated with and without inclusion of diabatic processes, with the surface fluxes in the diabatic forecasts generally computed from climatological SST fields. This may be viewed as an extreme form of SST anomaly experiment, in which the anomalous SST field was adjusted to reduce the air-sea temperature differences, and hence the surface heat fluxes, to zero everywhere. The differences between such parallel forecasts are probably representative of the maximum effects that one can expect from natural SST variations, for it seems reasonable that differences between zero and non-zero surface fluxes will, in general, be larger than the differences due to local SST anomalies of a few degrees, such as are commonly found in nature.

One limited-area, short-range forecast experiment with and without ocean surface fluxes was carried out some years ago (Spar, et al., 1961) with a quasi-geostrophic model (Spar, 1962) on three cases of winter cyclogenesis off the east coast of the United States. This experiment indicated that coastal cyclones form and develop, at least during their first day, primarily as a result of the barocline structure of the atmosphere, and that only after cyclogenesis has occurred does the offshore flow of cold continental air become sufficiently vigorous to induce strong sea-air heat fluxes, which may then further modify the pressure field. On the other hand, numerical experiments with cases of cyclogenesis off the Asiatic coast by the Japan Meteorological Agency (1965) have shown that, over a 3 day forecast period, diabatic processes played a prominent role in cyclogenesis and improved the forecasts. Although the relative contributions of surface flux and latent heat release to the diabatic predictions were not explicitly separated in the latter experiments, the magnitudes of the surface heat fluxes were shown to be quite large, and they undoubtedly did have a significant influence on the atmosphere.

It is, of course, reasonable to expect that surface heat fluxes as high as a kilolangley day$^{-1}$ or more, which are not uncommon in winter off the east coasts of North America and Asia and in the Gulf of Alaska, should produce significant effects on the vorticity and pressure fields. As shown, for example, by Winston (1955) and Pyke (1963), there is ample evidence that such fluxes may be primary causes of cyclogenesis in the Gulf of Alaska. The influence of oceanic surface heat fluxes on cyclone development has also been documented by Petterssen, et al. (1962) in a diagnostic study, and by Miyakoda, et al. (1969) in prognostic experiments with a 9-level primitive equation hemispheric model.

The physical influence of surface heat flux over the ocean thus appears to be fairly well understood, and its importance in short-range weather prediction is hardly a matter for dispute. From the viewpoint of long-range forecasting development, it is furthermore clear that the effects of persistent large-scale SST anomalies on the surface fluxes cannot be ignored. There is, however, an intermediate problem about which less is known, and that is the influence of temporal SST variations on forecast quality in the short and extended ranges. With regard to this problem, several questions are still unanswered. For example, how sensitive are current prediction and general circulation models to real variations, as well as errors, in the SST fields? Will the use of observed SST values rather than climatological (or other time-averaged) values lead to forecast improvement in the short range (1 to 3 days), or in the extended range (4 to 14 days)? It is, in fact, not known with any certainty how important it is to specify accurately, or to predict, the SST field for the purposes of short-range and extended weather prediction. The benefits, if any, gained from more accurate specification of the SST field could, for example, be completely overwhelmed by the decay of predictability by the time the diabatic effects of the ocean surface fluxes significantly affect the atmosphere.

An experiment was carried out at the NASA Goddard Institute for Space Studies (GISS) in New York City with the GISS 9-level global general circulation model (Somerville, et al., 1974) in an effort to answer these questions. In this experiment, three parallel forecasts were carried out for a two week period starting with "real" initial conditions over the globe on 20 December 1972. (The same case was used by Somerville, et al. (1974) to illustrate the forecast performance of the GISS model.) Two of the forecasts were computed, respectively, with climatological (December normal) and observed (20 December 1972) SST fields. The third, a predictability test, was computed using the climatological SST field, but with the initial atmospheric state altered by a random sprinkling of small errors.

The results of the experiment, which are described below, indicate that, at least for the model employed, which appears to be representative of the current "state of the art" (Druyan 1974), and for the SST anomalies of the case chosen for the experiment, the forecast quality is virtually unaffected by temporal variations of the SST field, and the model atmosphere is relatively insensitive to these variations up to about one week.

The reader is referred to Somerville, et al., (1974) for details of the primitive equation GISS model. It will be noted, however, that the model uses a spherical grid with a horizontal resolution of 4 degrees of latitude by 5 degrees of longitude.

## Data Set

Initial meteorological conditions for the experiment were derived from a global data set for 00 GMT 20 December 1972 provided by the National Meteorological Center (NMC), which also furnished the 12-hourly global data for the subsequent two-week period. (The initial sea-level pressure and 500-mb height fields for this case over the northwest quadrant, i.e., the western half of the Northern Hemisphere, were shown in Somerville, et al. (1974).) The climatological sea surface temperatures employed in the "control" forecast, here designated as the "C" run, were derived from the NCAR[4] monthly mean ocean temperature tabulation (Washington and Thiel, 1970) for the month of December. For the "anomaly" forecast, designated here as the "A" run, the monthly mean SST field in the Northern Hemisphere[5]

---

[4]National Center for Atmospheric Research

[5] Observed SST values were actually inserted as far south as latitude 18S. For the remainder of the Southern Hemisphere, due to the paucity of SST observations, climatological SST values were used for both the A and C runs.

was replaced by an "observed" SST field derived from a daily SST analysis provided through the courtesy of the Naval Fleet Numerical Weather Central in Monterey, California. All data were interpolated to the GISS 9-layer model structure and to the horizontal grid of 4 degrees of latitude by 5 degrees of longitude employed in the model.

The difference, in degrees Celsius (C), between the daily observed SST and the corresponding climatological monthly mean value, henceforth referred to as the SST anomaly, is shown for 20 December 1972 in Figure 1. While the SST anomaly field on this date does exhibit many small-scale irregularities, it also contains several coherent large-scale features, especially in the Pacific Ocean where the anomalies are predominantly positive. All the larger anomalies in the North Pacific, e.g. those in excess of 2C, are positive. Thus, for example, one finds in the eastern tropical region of the Pacific, an axis of positive anomalies along latitude 6N, with a maximum value of +3.4C at 6N, 120W. At higher latitudes, large positive anomalies are concentrated along the 42 nd parallel, with maxima of +3.6C in mid-ocean, at 42N, 150W, and +5.1C south of the Kurile Islands, at 42N, 155E between the mean positions of the Oyashio and Kuroshio Currents. At the position of Weather Ship "Papa", 50N, 145W, the SST anomaly on this date was only +0.4C. The largest negative anomaly in the North Pacific Ocean is -1.8C, to the west of San Francisco, at 38N, 125W in the center of a cold pool covering the extreme eastern region of the North Pacific from the subtropics to southern Alaska. In the North Atlantic Ocean the anomalies are predominantly negative, although there are also areas of positive anomalies, notably on the Equator and adjacent to the east coast of the United States.

Some indication of the persistence of the SST anomaly field in the North Pacific is provided by Figure 2 in which the SST anomalies are plotted for the period 15 December 1972 through 3 January 1973 at the 5 points mentioned above: 6N, 120W; 42N, 150W; 42N, 155E; 50N, 145W; 38N, 125W. (The anomalies for all 20 days are computed relative to the December mean SST.) The cold water west of San Francisco clearly remained cold for the 20 day period, with anomalies decreasing to a minimum of -2.6C. The warm equatorial pool at 6N likewise remained warm, the anomaly rising to more than +4C on 24 December before declining to a minimum of +2.2C at the end of the period. The positive anomaly at 42N in the eastern Pacific also weakened during the two week period after 20 December, reaching a low value of +2.3C, but the warm pool remained intact. On the other hand, the very large positive anomaly between the mean Kuroshio and Oyashio Current positions in the western Pacific decreased markedly after 20 December, from a maximum of +5.4C to a minimum of +1.1C, possibly reflecting temporal meandering of the ocean current systems.

Although the SST field was obviously not constant during the two week forecast period, its general configuration, especially over the Pacific Ocean, remained relatively steady. For this reason, and in order to simulate a realistic current operational forecast situation in which the SST field would ordinarily not be predicted, the sea temperatures for 20 December 1972 were held constant during the A run.

The predictability run, designated P, was intended to provide some measure of the inherent limits on predictability of the model. For the P run, the initial state of the atmosphere was altered by superimposing on it a random distribution of small errors. The root-mean-square (r.m.s.) magnitudes of these errors were 3 m $sec^{-1}$ in the wind velocity components of all levels, 1 degree C in the temperatures at all levels, and 3 mb in the sea level pressures. The climatological SST field was used for the P run. The C and A forecasts were computed for 14 days, and the P forecast was carried out for 12 days.

## Results

The results of the experiment have been analyzed both synoptically, by comparison of prognostic and observed maps, and numerically, mainly in terms of r.m.s. forecast errors and r.m.s. differences.

Although a variety of parameters were analyzed, including wind velocity, temperature, precipitation, sea-level pressure, and 500-mb height, the results are consistent for all parameters, and are therefore presented here only in terms of the last three quantities.

The local effect of the SST anomaly on the computed precipitation over the region of the oceanic anomaly itself is, as expected, a local enhancement of rainfall over warm water and a suppression of rainfall over cold water. To illustrate this convective effect, the computed rainfall amounts, in inches, were accumulated over a period of 13 forecast days and over all the 29grid points in the tropical eastern Pacific at which the positive SST anomalies were at least 2 degrees C.[6] For both the C and P runs, in both of which the climatological SST field was used, the cumulative rainfall computed was equal to approximately 20 units, while for the A run, based on the anomalous SST values, the cumulative precipitation computed for the same 29 grid points was more than 38 units, an increase of almost a factor of two. (Although the absolute values are of no physical significance, it may be noted that this represents an average increase of 0.05 inches per grid point per day.) A similar cumulative rainfall computation was also done for the same period for all the land grid points from 2N to 30N and 90W to 115W. For this region, which lies to the east and north of the warm SST anomaly, the cumulative precipitation amounts were 9 units for both the A and P runs and 11 units for the C runs, indicating no systematic remote effect of the anomaly on the predicted rainfall.

There is, of course, no reliable means of verifying either quantitative or qualitative precipitation forecasts over the ocean. However, the effect of the SST field on the skill of the precipitation forecasts was

---

6 Unfortunately, it was not possible to do the opposite experiment, illustrating suppression of convection by cold anomalies, because there were too few points at which negative anomalies of this magnitude could be found in the Northern Hemisphere.

evaluated over North America[7], including adjacent ocean areas, in terms of the cumulative percent correct of the daily qualitative (rain or no-rain) precipitation forecasts over a 13-day period. Each 24-hour forecast in the Series, was computed from the same 20 December 1972 initial state and verified against the daily precipitation as reported by the National Weather Service and interpolated to the GISS grid. A subset of 57 grid points at which reliable estimates could be made by the precipitation was used for the verification, and the percent correct scores were accumulated over days 1 through 13. As shown in Table 1, the use of the 20 December observed SST field, represented by run A, did not result in any improvement over the precipitation forecasts based on the climatological SST values represented by run C. In fact, the skill is somewhat less for the A run. The effect of initial random error on the precipitation forecasts, however, as indicated by the differences between the values for runs C and P, was even larger than that due to the SST anomaly. Thus, no significance should be attached to the differences between colums A and C in Table 1.

Table 1. Cumulative percent correct of 24-hour qualitative precipatation forecasts (rain or no-rain) at 57 grid points in the North American region. Scores are accumulated progressively over 13 forecast days. All forecasts were calculated from initial meteorological conditions at 00GMT, 20 December 1972, and verified against daily National Weather Service observations. C, A, and P represent the control, anomaly, and predictability runs, respectively. (See text for explanation).

---

7 The region used for this evaluation lies between latitudes 30N and 58N and longitudes 70W and 125W.

| Day | C | A | P | No. of Forecasts (grid points x days) |
|---|---|---|---|---|
| 1 | 75 | 74 | 77 | 57 |
| 2 | 77 | 74 | 74 | 114 |
| 3 | 75 | 73 | 70 | 171 |
| 4 | 72 | 71 | 68 | 228 |
| 5 | 69 | 69 | 65 | 285 |
| 6 | 67 | 67 | 64 | 342 |
| 7 | 64 | 64 | 63 | 400 |
| 8 | 63 | 63 | 62 | 457 |
| 9 | 62 | 62 | 60 | 514 |
| 10 | 60 | 59 | 58 | 571 |
| 11 | 60 | 59 | 58 | 628 |
| 12 | 59 | 57 | 57 | 685 |
| 13 | 57 | 56 | 56 | 742 |

The influence of the SST anomaly on the daily computed sea-level pressure field over the two-week forecast period was computed for various spatial domains, including the globe, the Northern Hemisphere, and various continental areas. However, as the results are essentially the same for all regions, they can be illustrated adequately by Figures 3 and 4, which are for Europe and the North American continent respectively. The upper three curves in the two figures show the growth of r.m.s. forecast errors, in millibars (mb), for thr three appropriately labeled forecast runs[8]. It is apparent from the curves for C and A that no significant differences in the r.m.s. errors resulted from the SST variations. During the first week the error growth is almost identical for both runs over both continents, while in the second week the differences between A and C runs are not consistent over the two continents. Clearly, the use of the observed SST field did not improve the sea level pressure forecasts over either the short or extended range.

---

8 The r.m.s. errors and differences were computed for every 12 hours of the two week forecast period.

The error curves for the P run also exhibit almost the same growth rate as the other two, at least during the first week. It is interesting to note that the initial r.m.s. sea level pressure error of approximately 3 mb in the P case apparently has no discernible effect on the growth of the r.m.s. error curve, and that, after 12 to 24 hours, all three predictions exhibit almost the same r.m.s. errors in the sea-level pressure field. The same absence of influence of the initial random errors on the growth of the r.m.s. forecast error is also found in the other parameters and regions studied. In all instances, the prediction error overtakes the initial random error within 12 to 24 hours, after which the r.m.s. errors for all runs grow at about the same rate. Apparently the small-scale initial random error field decays rapidly during the forecast computation, while the larger-scale forecast error field grows.

The two lower curves in Figures 3 and 4, illustrating the sensitivity of the model atmosphere to SST anomalies and random initial errors, represent the daily r.m.s. sea level pressure differences between the A and C runs on the one hand and the P and C runs on the other. These curves show the effects of the SST anomaly and initial random error fields on the computed meteorological histories, rather than their effects on the quality of the forecasts. From the C-A curves, it can be seen that the effect of the SST anomaly on the predicted sea-level pressure field grows quite slowly during the first week. Thus, after 7 days the r.m.s. differences between A and C are no larger than the r.m.s. errors that developed within the first 12 hours in the sea-level pressure forecasts.

The r.m.s. differences between P and C in Figures 3 and 4 decay rapidly during the first 24 hours, as the effect of the small-scale initial error perturbation is apparently smoothed out during the prognostic computation. (This result is consistent with the nearly constant value of the r.m.s. forecast error in the P run noted above during the first 24 hours.) However, after the first day, the r.m.s. sea-level pressure difference due to the initial error field grows at approximately the same slow rate as does the difference due to the SST anomaly. Essentially the same results are found also over the oceans and over the entire Northern Hemisphere.

After the first week, the r.m.s. sea-level pressure differences due to either SST anomalies or random errors grow more rapidly; but by then, as indicated by the magnitudes of the r.m.s. forecast errors, the computed fields clearly have no predictive value. Obviously, the influence of either SST variations or random initial errors on the computed daily sea-level pressure fields during the two-week forecast period is relatively insignificant compared with the growth of prediction error. Furthermore, the effect of the SST anomalies is no greater than that resulting from random errors in the initial meteorological fields.

Figure 5 further illustrates the response of the model atmosphere to SST anomalies and random errors in terms of the predicted 500-mb height field over the Northern Hemisphere. As in Figures 3 and 4, the upper three curves represent the r.m.s. forecast errors, plotted every 12-hours, for the C, A, and P runs, while the lower two curves show the r.m.s. differences between A and C and P and C respectively. The results for the 500-mb heights are clearly the same as for sea-level pressures. Again, there is no discernible influence of the SST anomaly field on the general quality of the forecasts as represented by r.m.s. errors, and the influence of the SST anomaly is small compared with the growth of prediction error, being no larger than that due to random initial errors.

A synoptic representation of the influence of the SST anomalies on the predicted sea-level pressure field is shown in Figure 6 for the northwest quadrant of the earth. Isobars of forecast error, drawn for an interval of 5 mb, are displayed for both the C and A runs for forecast periods of 1, 3, and 6 days. For each day, while the magnitudes of the errors grow, the error fields are virtually identical for the two runs. In fact, maps of differences of the errors between A and C show mainly zero values, and are therefore not reproduced here. Prognostic synoptic maps of 500 mb heights and 850 mb temperatures were also compared and found to be virtually identical for the A and C forecasts.

Although, as shown above, the SST anomalies have no significant influence on the quality of the daily forecast fields over a two week forecast period, it is possible that the thermal forcing associated with these anomalies may have a greater influence on the tine-averaged state of the atmosphere. To test this possibility, 14-day averages of observed and predicted fields of sea-level pressure and 500-mb height were computed for the three forecast runs. The results of this study are presented below in terms of synoptic maps and r.m.s. errors.

The 14-day mean sea level pressure fields forecast by the Control (C) and Anomaly (A) runs, together with the corresponding observed fields are shown in Figure 7 for the northwest and northeast quadrants. No significant differences between the C and A forecast fields are apparent. In the Atlantic the two forecasts are equally satisfactory, the principal error in both being the failure to forecast a sufficiently deep Icelandic Low. In the western Pacific both C and A failed to forecast the depth of the low in the Gulf of Alaska and the trough extending southward from it. Similarly both C and A failed to forecast the strength of the Eurasian high pressure system and the depth of the low pressure system in the Arctic Sea to the north, although both did adequately predict the general configuration of the pressure field.

Figure 8 illustrates the 14-day mean 500-mb height fields forecast by the Control (C) and Anomaly (A) runs, together with the corresponding observed fields. In the northwest quadrant, the two predicted 500 mb mean fields are almost identical. Both C and A failed to forecast the strong ridge off the California coast and the trough to the west, as well as the northeast-southwest trough across the United States. On the other hand, both forecasts were equally satisfactory over the Atlantic. In the northeast quadrant, the forecasts were also almost identical. Both failed to predict the amplitude of the trough-ridge system over Eurasia east of the Black Sea, but the forecast mean maps were otherwise equally satisfactory.

Root-mean-square (r.m.s.) forecast errors in the 14-day mean fields are shown in Table 2 for the 500-mb level heights, in meters, and the sea level pressures, in millibars. The four forecasts compared are (C) the Control forecast, (A) the Anomaly forecast, (P) the Predictability forecast, and (R) a persistence forecast. The persistence forecast is simply the observed field, from the NMC analysis, for 00 GMT 20 December 1972. The forecasts are compared for four areas of the earth: the total globe between latitudes 86N and 86S, the Northern Hemisphere from 2N to 86N, the European land area between latitudes 34N and 86N and longitudes 10W and 40E, the western United States land area between latitudes 30N and 54N and longitudes 95W and 130W, and the North American land area between latitudes 30N and 70N and longitudes 75W and 130W.

From Table 2 it is apparent that the Anomaly forecast (A) made with the "observed" SST field is not consistently superior to either the Control forecast (C), made with the climatological SST field, or the Predictability forecast (P) made from an error-perturbed initial state and the climatological SST field. All three mean sea level pressure forecasts are far better than persistence over North America (including the western United States), and are also clearly superior to persistence over the Northern Hemisphere. On the other hand, the three sea level pressure forecasts are inferior to persistence over Europe. At the 500-mb level, the three forecasts for Europe again fail to beat persistence, while over North America (including the western United States), where the Predictability Forecast (P) was actually best, the Control forecast (C) also was poorer than persistence.

Table 2. Root-mean-square (r.m.s.) forecast errors in (I) mean 500-mb heights (meters) and (II) mean sea level pressures (millibars) for the two-week period beginning 20 December 1972. C, A, and P denote the Control, Anomaly, and Predictability forecasts, and R represents a persistence forecast. (See text for details.) The "best" forecast in each case is underlined.

I. 500-mb height (m)

| Area | C | A | P | R |
|---|---|---|---|---|
| Globe | 75.0 | 73.3 | 75.4 | 75.7 |
| Northern Hemisphere | 66.9 | 64.8 | 68.0 | 79.5 |
| Europe | 128. | 123. | 135. | 108 |
| Western U.S. | 66.8 | 50.9 | 43.4 | 51.1 |
| North America | 69.7 | 59.8 | 57.0 | 68.3 |

II. Sea level pressure (mb)

| Area | C | A | P | R |
|---|---|---|---|---|
| Globe | 6.89 | 7.01 | 6.93 | 7.23 |
| Northern Hemisphere | 6.21 | 6.09 | 6.26 | 7.61 |
| Europe | 8.12 | 7.54 | 8.43 | 6.85 |
| Western U.S. | 2.74 | 3.34 | 3.26 | 5.08 |
| North America | 3.23 | 3.99 | 3.37 | 5.15 |

## Summary

From the single experiment described above one can draw, at best only preliminary conclusions. Further extended range prediction experiments are necessary, and are being carried out at GISS and elsewhere. Nevertheless it is probably useful to document the current state of the art at this time, even though it will undoubtedly be necessary to supplement and correct this report as additional experiments are performed and as models are further developed.

The GISS model is sensitive to SST anomalies in the sense that convective precipitation forecast by the model is locally enhanced over the ocean in regions of moderately large positive SST anomalies. (Cold anomalies undoubtedly suppress convective precipitation in the model, but the data on cold cases were not sufficient to demonstrate this point.) However, while it was not possible to evaluate the effect of this enhancement on the quality of the forecasts over the ocean, the use of the observed rather than the climatological SST field had no positive effect on the quality of the precipitation forecasts over continental areas where the forecasts could be verified.

The mass fields forecast by the model, as represented by sea level pressures and 500-mb heights, are relatively insensitive to variations in sea temperatures. Effects of the SST anomalies grow very slowly for about a week compared with the rapid growth of prediction error. At the end of a week, the r.m.s. differences between forecasts made with and without SST anomalies are no larger than the corresponding r.m.s. forecast errors that developed within the first 12 to 24 hours. The effects of SST anomalies grow very slowly for about a week compared with the rapid growth of prediction error. At the end of a week, the r.m.s. differences between forecasts made with and without SST anomalies are no larger than the corresponding r.m.s. forecast errors that developed within the first 12 to 24 hours. The effects of SST anomalies, like those due to initial random errors in the atmospheric fields, do grow much faster after the first week, but by then the daily forecast fields have no predictive value. An interesting sidelight of the experiment is the fact that the influence of random initial atmospheric errors decays rapidly within the first day of prediction compared with the growth of forecast error, but then grows at about the same rate as the effect of SST anomalies over the two week period.

Daily prognostic synoptic maps of sea level pressure and 500-mb height (as well as 850-mb temperature) are found to be virtually identical for about a week whether computed with climatological or observed SST fields. Similarly, prognostic 14-day mean maps of sea level pressure and 500-mb height (as well as 850-mb temperature) are also almost indistinguishable whether computed with climatological or observed SST fields.

Provisionally, the experiments appear to suggest that observed SST fields contribute little or nothing to the improvement of forecast quality in the short and extended ranges. Any possible benefits gained from more accurate specification of the SST field appear to be overwhelmed by the decay of predictability before the diabatic effects associated with the SST anomalies are felt by the atmosphere. However, it should be noted that anomalies of larger magnitude than those used in this experiment do occur in nature and may have larger effects; that the GISS model may be too insensitive to surface fluxes and their anomalies; and that smaller scale anomalies, such as those associated with regions of large SST gradients (e.g., Gulf Stream meanders and eddies), may have more significant effects in a forecast computed with higher spatial resolution.

## Acknowledgements

The authors wish to thank Robert Jastrow, director of GISS, Leonard Druyan, Milton Halem, William Quirk, Richard Somerville, and the staff of the Goddard Institute for Space Studies for their unstinting cooperation in the performance of this study. We are also grateful to the National Meteorological Center (National Weather Service, National Oceanic and Atmospheric Administration, Department of Commerce) for providing the 14-day meteorological data set, to the Naval Fleet Numerical Weather Central for the daily sea surface temperature data, and to the National Center for Atmospheric Research for the climatological SST data.

# REFERENCES


Bjerknes, J., 1966: A possible response of the atmospheric Hadley circulation to equatorial anomalies of ocean temperature. Tellus, 18, 820-829.

Bjerknes, J., 1969: Atmospheric teleconnections from the equatorial Pacific. Monthly Weather Review, 97, 163-172.

Bushby, F. H. and M. K. Hinds, 1955: Further computations of 24-hr pressure changes based on a two-parameter model. Quarterly Journal of the Royal Meteorological Society, 81, 396-402.

Druyan, L. M., 1974: Short range forecasts with the GISS model of the global atmosphere. Monthly Weather Review, 102, 269-279.

Houghton, D. D., J. E. Kutzbach, M. McClintock and D. Suchman, 1974: Response of a general circulation model to a sea temperature perturbation. Jour. of Atmos. Sci., 31, 857-868.

Japan Meteorological Agency, Electronic Computation Center, 1965: 72-hour baroclinic forecast by the diabatic quasi-geostrophic model. Journal of the Meteorological Society of Japan, 43, 246-261.

Manabe, S. and K. Bryan, 1969: Climate calculations with a combined ocean - atmosphere model. Journal of the Atmospheric Sciences, 26, 786-789.

Miyakoda, K., J. Smagorinsky, R. F. Strickler and G. D. Hembree, 1969: Experimental extended predictions with a nine-level hemispheric model. Mo. Wea. Rev., 97, 1-76.

Namias, J., 1962: Influences of abnormal surface heat sources and sinks on atmospheric behavior. Proceedings of the International Symposium on Numerical Weather Prediction, Tokyo, Japan, November 7-13, 1960. Meteorological Society of Japan, pp. 615-627.

Namias, J., 1969: Seasonal interactions between the North Pacific Ocean and the atmosphere during the 1960's. Monthly Weather Review, 97, 173-192.

Namias, J., 1970: Macroscale variations in sea-surface temperatures in the North Pacific. Journal of Geophysical Research, 75, 565-582.

Namias, J., 1971: The 1968-69 winter as an outgrowth of sea and air coupling during antecedent seasons. Journal of Physical Oceanography, 1, 65-81.

Petterssen, S., D. L. Bradbury and K. Pedersen, 1962: The Norwegian cyclone models in relation to heat and cold sources. Geofys. Publikas., 24, 243-280.

Pyke, Charles B., 1965: On the role of air-sea interaction in the development of cyclones. Bull. of the Amer. Meteor. Soc., 46, 4-15.

Ratcliffe, R. A. S., 1973: Recent work on sea surface temperature anomalies related to long-range weather forecasting. Weather, 28, 106-117.

Reed, R. J., 1958: A graphical prediction model incorporating a form of nonadiabatic heating. Journal of Meteorology, 15, 1-8.

Rowntree, P. R., 1972: The influence of tropical East Pacific Ocean temperatures on the atmosphere. Quart. Journ. Roy. Meteor. Soc., 98, 290-321.

Sawyer, J. S., 1965: Notes on possible physical causes of long-term weather anomalies. WMO Tech. Note No. 66, Geneva, pp. 227-248.

Somerville, R. C. J., P. H. Stone, M. Halem, J. E. Hansen, J. S. Hogan, L. M. Druyan, G. Russell, A. A. Lacis, W. J. Quirk and J. Tenebaum, 1974: The GISS model of the global atmosphere. Journ. Atmos. Sci., 31, 84-117.

Spar, J., J. P. Gerrity, Jr., and L. A. Cohen, 1961: Some results of experiments with an integrated, wet, diabatic weather prediction model. Scientific Report No. 2, Contract Nonr - 285(09). Research Division, New York University. 28 pages.

Spar, J., 1962: A vertically integrated wet, diabatic model for the study of cyclogenesis. Proceedings of the International Symposium on Numerical Weather Prediction in Tokyo, Japan, November 7-13, 1960. Meteorological Society of Japan, pp. 185 - 204.

Spar, J., 1973 (a): Some effects of surface anomalies in a global general circulation model. Mo. Wea. Rev., 101, 91-100.

________, 1973 (b): Transequatorial effects of sea surface temperature anomalies in a global general circulation model. Mo. Wea. Rev., 101, 554-563.

________, 1973 (c): Supplementary notes on sea surface temperature anomalies and model generated meteorological histories. Mo. Wea. Rev., 101, 767-773.

Washington, W. M. and L. G. Thiel, 1970: Digitized monthly mean ocean temperatures over the globe. Tech. Note 54, National Center for Atmospheric Research, Boulder, Colo. 30 pages.

White, W. S., and A. E. Walker, 1973: Meridional atmospheric teleconnections over the North Pacific from 1950 to 1972. Monthly Weather Review, 101, 817-822.

Winston, J. S., 1955: Physical aspects of rapid cyclogenesis in the Gulf of Alaska. Tellus, 7, 481-500.

## FIGURES

Fig. 1. Sea surface temperature anomalies, in degrees Celsius, over the Northern Hemisphere based on data provided by the Naval Fleet Numerical Weather Central for 20 December 1972. The dotted curves are zero anomaly isotherms. Solid curves denote positive anomalies and dashed curves indicate negative anomalies: C and W denote cold and warm centers.

Fig. 2. Selected daily sea surface temperature anomalies in the North Pacific Ocean during the period 15 December 1972 - 3 January 1973.

Fig. 3. Root-mean-square (r.m.s.) errors in sea level pressures (mb) over Europe generated by Control (C), Anomaly (A) and Predictability (P) forecasts for the two week period beginning OOGMT, 20 December 1972. Also shown are the r.m.s. differences in sea level pressure between the P and C and the A and C forecasts for the same period.

Fig. 4. Same as figure 3, but for North America

Fig. 5. Root-mean-square (r.m.s.) errors in 500-mb heights (meters) over the Northern Hemisphere generated by Control (C), Anomaly (A), and Predictability (P) forecasts for the two week period beginning OOGMT 20 December 1972. Also shown are the r.m.s. differences in 500-mb height between the P and C and the A and C forecasts for the same period.

Fig. 6. Errors in forecast sea level pressure over the northwest quadrant on days 1, 3, and 6 after 20 December 1972. C and A denote the Control and Anomaly forecasts respectively. Error isobars are drawn for an interval of 5 mb.

Fig. 7. Forecast and observed mean sea level pressure fields over the Northern Hemisphere for the 14-day period beginning OOGMT, 20 December 1972. The Control and Anomaly forecasts are shown at the top and center, respectively, and the observed fields are at the bottom. Isobars are drawn for an interval of 5 mb.

Fig. 8. Forecast and observed mean 500-mb height fields over the Northern Hemisphere for the 14-day period beginning OOGMT, 20 December 1972. The Control and Anomaly forecasts are shown at the top and center, respectively, and the observed fields are at the bottom. Contours are drawn for an interval of 60 meters.

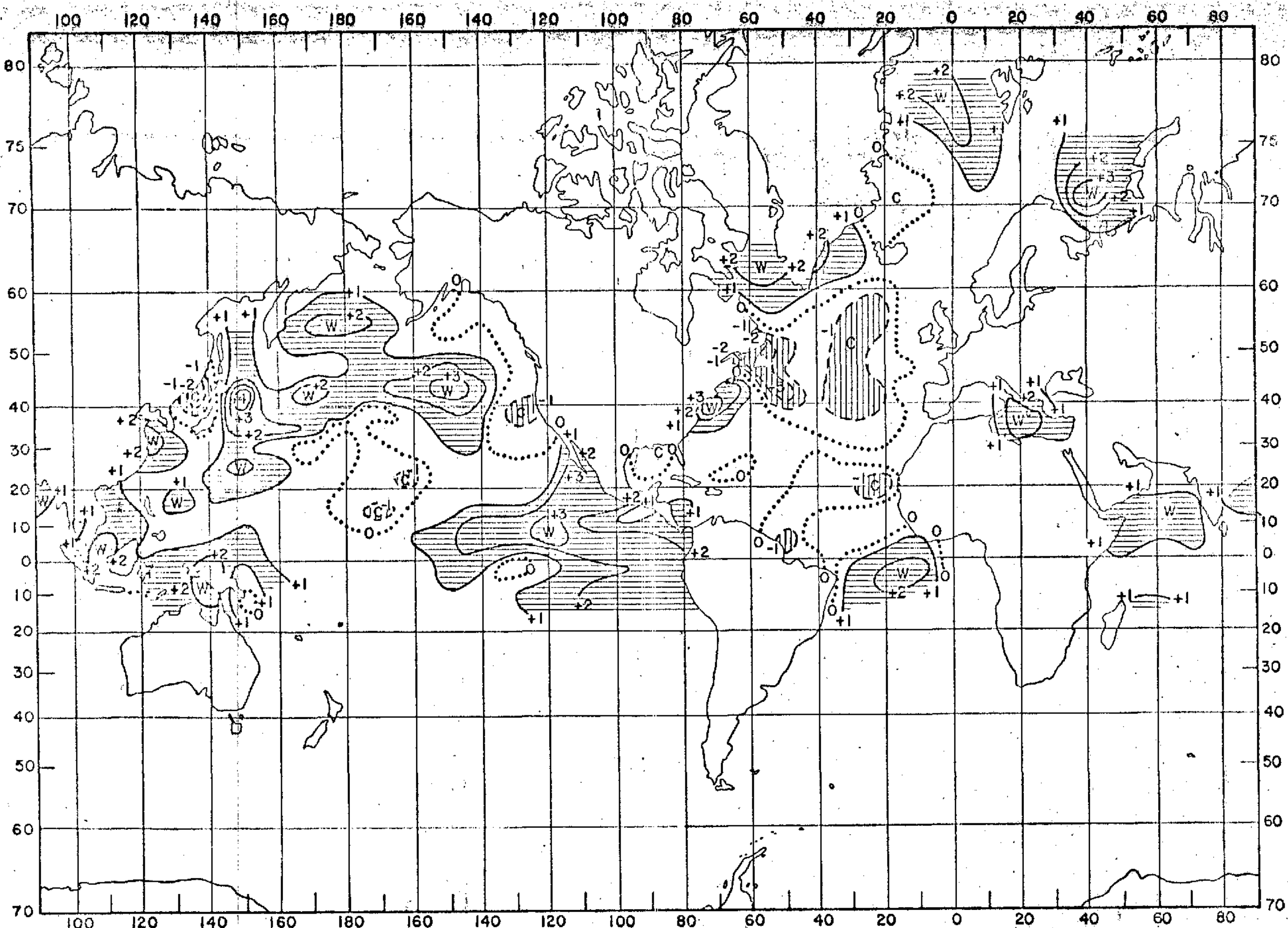

1

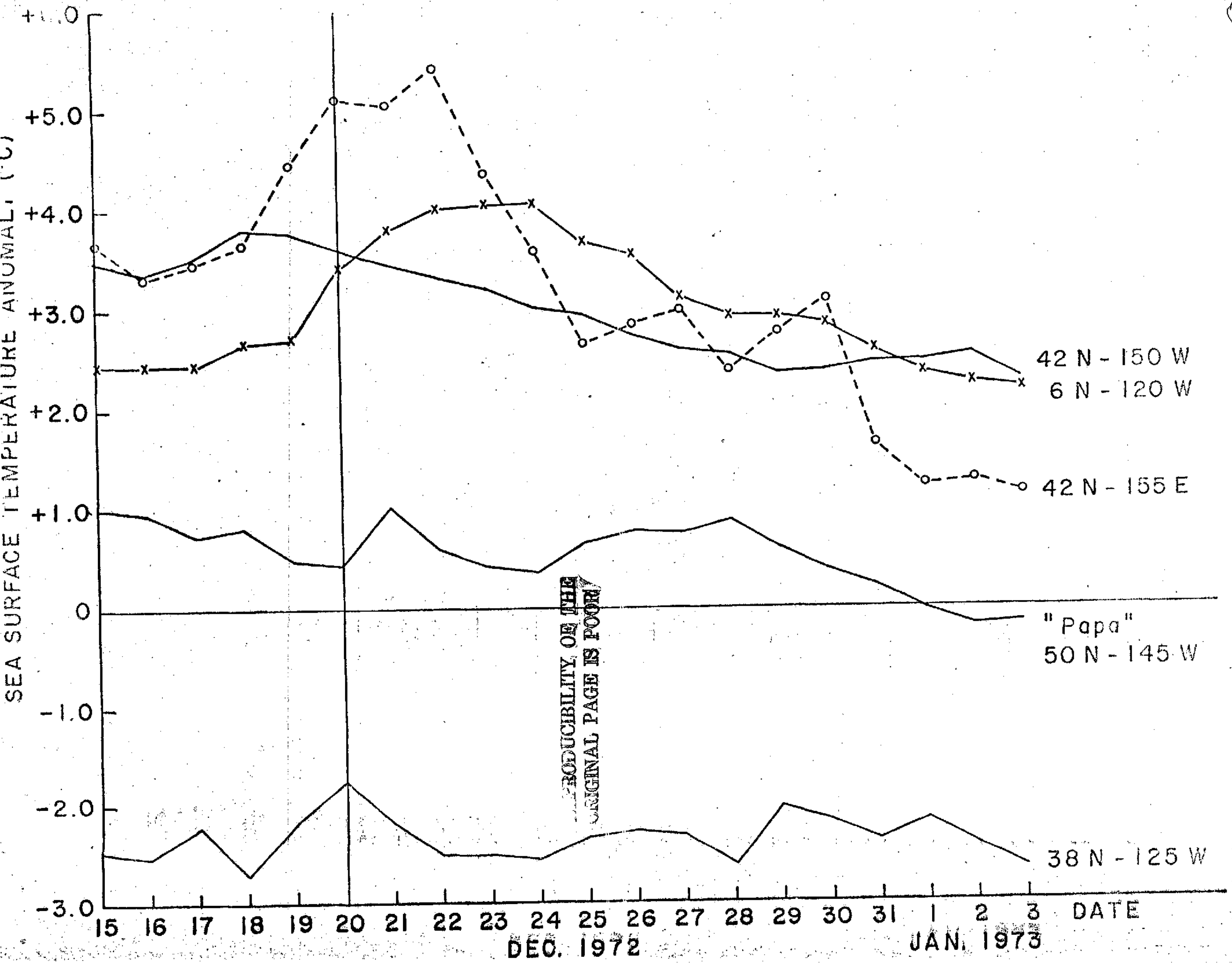
SEA SURFACE TEMPERATURE ANOMALY (°C)
+5.0
+4.0
+3.0
+2.0
+1.0
0
-1.0
-2.0
-3.0
42 N - 150 W
6 N - 120 W
42 N - 155 E
"Papa"
50 N - 145 W
38 N - 125 W
15 16 17 18 19 20 21 22 23 24 25 26 27 28 29 30 31 1 2 3 DATE
DEC. 1972
JAN. 1973

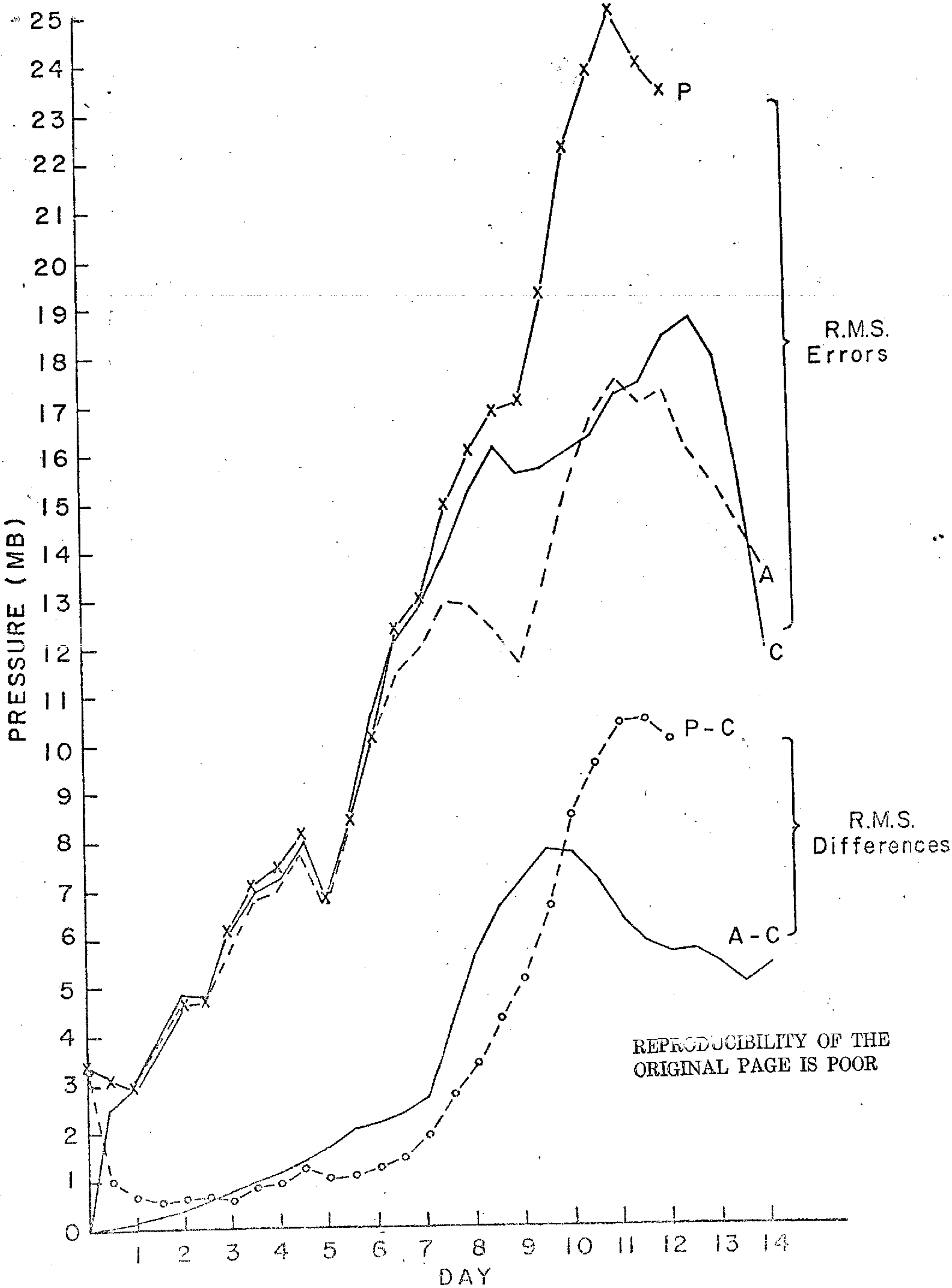

PRESSURE (MB)
DAY
P
A
C
P - C
A - C
R.M.S.
Errors
R.M.S.
Differences
0
1
2
3
4
5
6
7
8
9
10
11
12
13
14
15
16
17
18
19
20
21
22
23
24
25

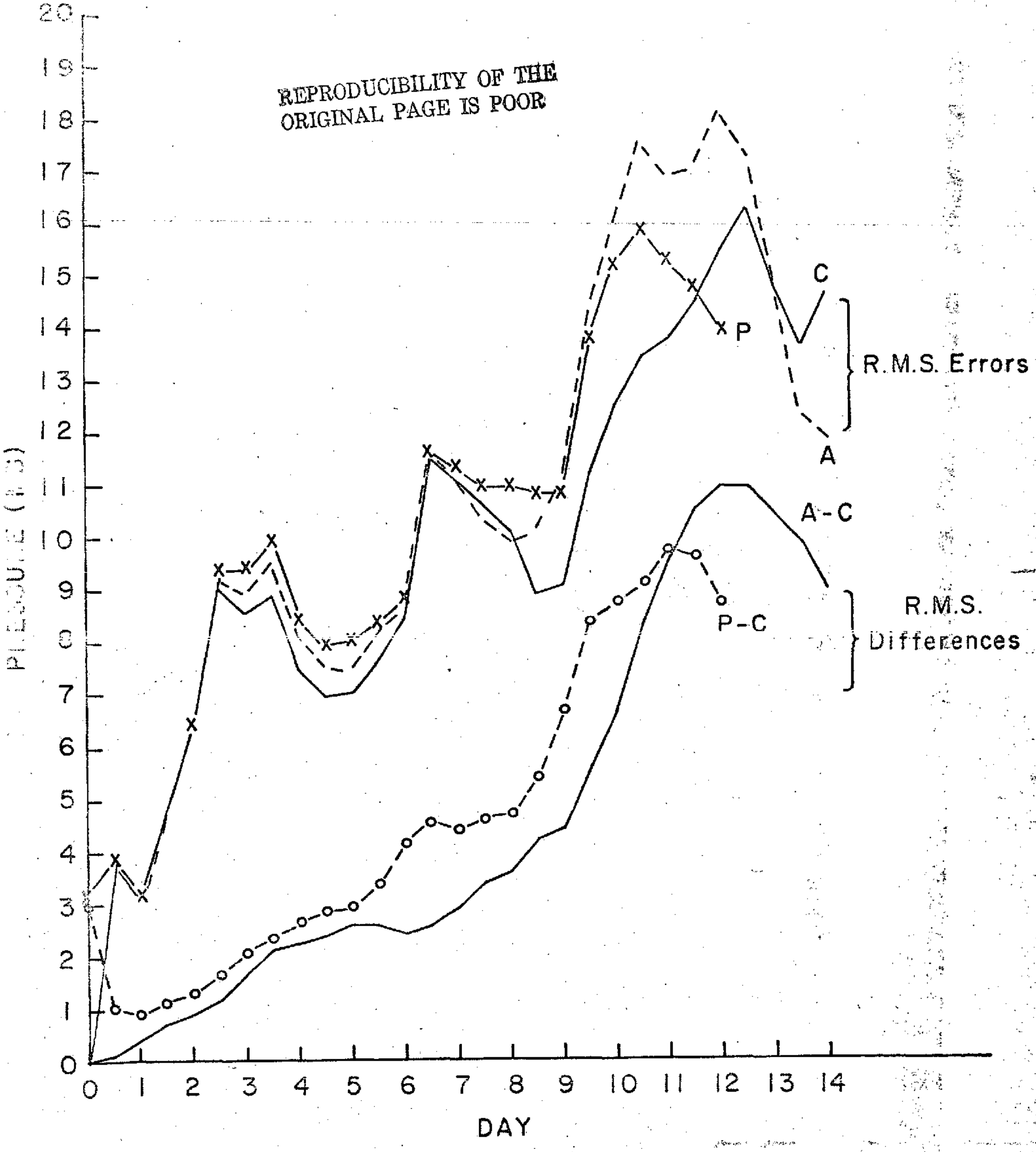

C
P
A
R.M.S. Errors
A-C
P-C
R.M.S. Differences
PRESSURE (MB)
DAY
0
1
2
3
4
5
6
7
8
9
10
11
12
13
14
15
16
17
18
19
20

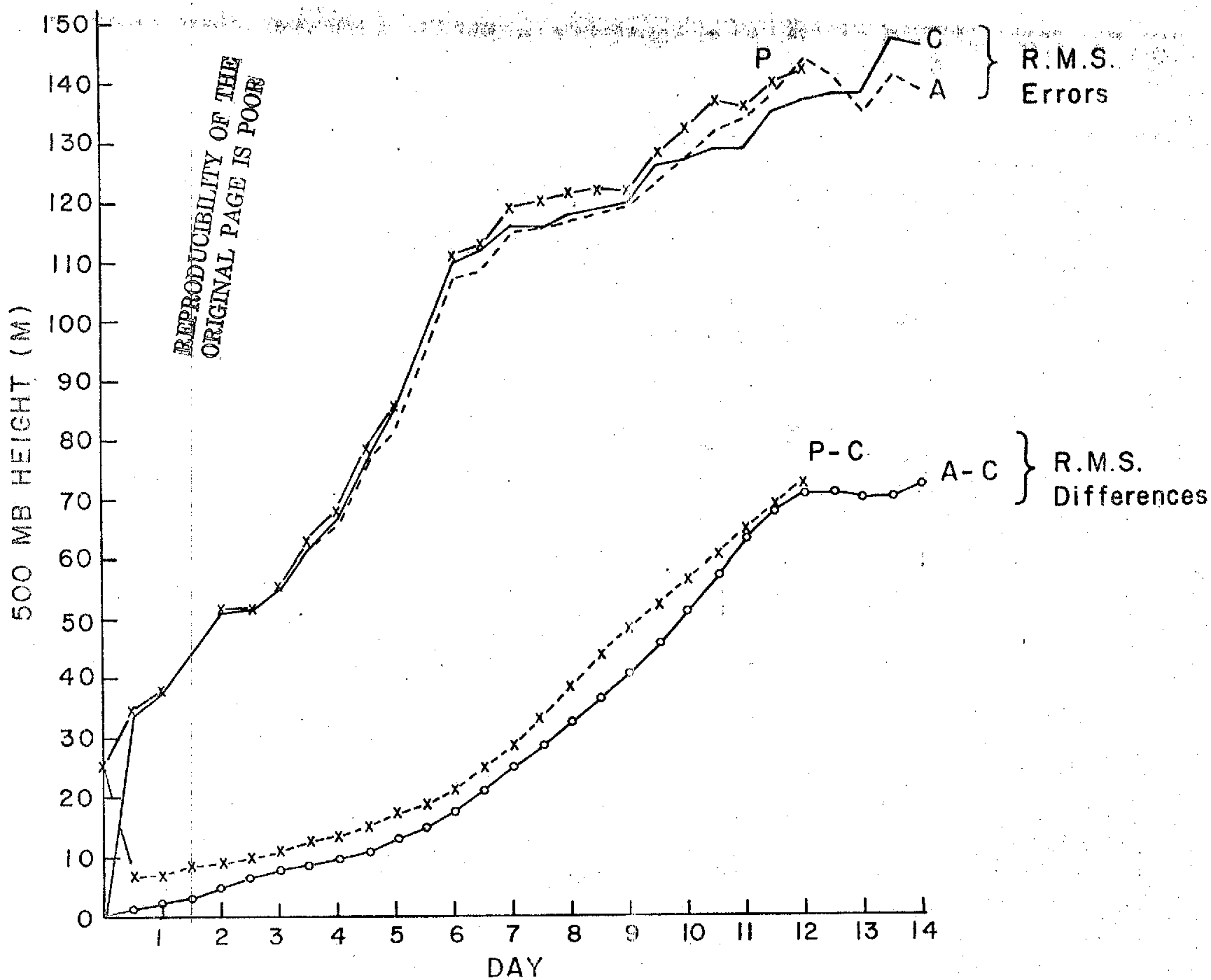
500 MB HEIGHT (M)
0
10
20
30
40
50
60
70
80
90
100
110
120
130
140
150
DAY
1 2 3 4 5 6 7 8 9 10 11 12 13 14
P
C
A
R.M.S. Errors
P-C
A-C
R.M.S. Differences